

### **Supplementary Figures Legends**

#### **Figure S1. *Prdm16* expression during mouse cerebral cortex development. Related to Figure 1.**

(A) *In situ* hybridization shows *Prdm16* expression during mouse embryonic and postnatal cortical development. Arrow at embryonic day 10.5 indicates the dorsal telencephalon, which gives rise to the cerebral cortex. *Prdm16* expression is high in the ventricular zone at all stages examined.

(B) Immunostaining for PRDM16 and NEUN in the cerebral cortex of newborn mice indicate that *Prdm16* is not expressed in cortical neurons.

(C) Immunostaining for PRDM16 and S100 $\beta$  indicates expression of *Prdm16* in cortical astrocytes at post-natal day 15.

Scale bars: 50  $\mu$ m (B, C).

**Figure S2. PRDM16 controls the laminar organization of the cerebral cortex. Related to Figure 2.**

(A) PRDM16 Immunostaining of E15.5 cKO cortex. Inset indicates the region shown at higher magnification in the three panels on the right. Reduction of PRDM16 signal is specifically observed in the ventricular zone. LGE: lateral ganglionic eminence; ChP: choroid plexus.

(B) The size of WT and *Prdm16* cKO cortex was compared at post-natal day 2 (P2) by measuring the length of the antero-posterior (A-P) and medio-lateral (M-L) axes.

(C) Upper images show immunostaining for SATB2<sup>+</sup> callosal projection neurons in WT and cKO cortex at P15. The total number of callosal neurons in hemisphere sections is not affected in the cKO cortex (refer to Figure 2A). Middle images show ROR $\beta$ <sup>+</sup> layer IV neurons and TBR1<sup>+</sup> layer V-VI neurons in WT and cKO cortex at P15. Lower images show VGLUT2<sup>+</sup> barrels in layer IV of the somatosensory cortex of WT and cKO brains at P10.

(D) Most cells forming heterotopias in the cKO cortex are BRN2<sup>+</sup>/CTIP2<sup>-</sup> upper layer-like neurons.

(E) Quantification of S100 $\beta$ <sup>+</sup> cells in WT and *Prdm16* cKO cortex at P15.

Results represent mean  $\pm$  SD; statistical analysis is unpaired Student's t test (n.s., not significant). Scale bars: 250  $\mu$ m (A, low magnification), 50  $\mu$ m (A, high magnification), 1 mm (B), 500  $\mu$ m (C, upper and middle images) and 100  $\mu$ m (C, lower images and D, E).

**Figure S3. Lineage-autonomous control of upper layer neuron position by PRDM16. Related to Figure 2.**

(A) Representative images of radial glia basal processes visualized by NESTIN immunostaining in E16.5 WT and *Prdm16* cKO cortex. Nuclear staining with DAPI was used to identify the

cortical plate (CP). Basal processes of radial glia extending across the CP and contacting the pial surface of the tissue are clearly seen in WT and *Prdm16* cKO brains. At this stage of development, the CP in cKO brains is thinner than in WT brains (white dashed line).

(B) *In utero* electroporation (IUE) of scrambled RNA and *Prdm16* shRNA into E14.5 WT brains.

At E17.5, cells co-electroporated with *Prdm16* shRNA and nuclear *GFP* show reduced PRDM16 levels in the ventricular zone in comparison to cells electroporated with scrambled RNA control (arrows).

(C) *In utero* electroporation of scrambled RNA and *Prdm16* shRNA into E14.5 WT brains and analysis of upper layer neuron migration at postnatal day 5 (P5). A plasmid driving constitutive expression of nuclear *GFP* was co-electroporated to label the progeny of radial glia. White boxes indicate the white matter and the presence of ectopic CUX1<sup>+</sup> upper layer neurons after *Prdm16* knockdown. Quantification is shown for *Prdm16* shRNA (n=4) and scrambled RNA (n=3).

(D) *Nex<sup>Cre</sup>* mice were crossed with a reporter mouse line carrying the *Rosa26<sup>lox-stop-lox-tdTomato</sup>* allele to confirm Cre-mediated recombination in cortical neurons in the intermediate zone (IZ) and cortical plate (CP). Recombination was not observed in the ventricular zone (VZ) and subventricular zone (SVZ).

(E) Electroporation of a plasmid encoding nuclear GFP (nGFP) into E15.5 WT and *Nex<sup>Cre</sup>*; *Prdm16* cKO cortex and analysis of upper layer neuron migration at P10. Representative images of WT cortex (n=3) and *Nex<sup>Cre</sup>*; *Prdm16* cKO cortex (n=5) show normal migration of electroporated neurons into upper cortical layers.

Results represent mean ± SD; statistical analysis is unpaired Student's t test (\*\*\*) p < 0.001).

Scale bars: 50 μm (A), 20 μm (B), 100 μm (C, D), 200 μm (E).

**Figure S4. Abnormal axonal projections in *Prdm16* cKO cortex. Related to Figure 2.**

(A) A plasmid encoding membrane tdTomato and nuclear GFP was electroporated into E15.5 WT and cKO cortex and axonal projections were analyzed at post-natal day 10 (P10).

(B) Coronal sections of electroporated WT and cKO cortex at the rostro-caudal levels indicated with red lines (I and II) in panel (A).

(C) Quantification of ipsilateral and contralateral axonal projections in WT (n=3 brains) and cKO cortex (n=4) at rostro-caudal level II. The corrected fluorescent intensity of axonal projections was quantified in the areas indicated on panel (B).

Results represent mean  $\pm$  SEM; statistical analysis is unpaired Student's t test (\*\*p < 0.01).

Scale bar: 400  $\mu$ m.

**Figure S5. Analysis of radial glia number and timing of neurogenesis. Related to Figure 3.**

(A) Total number of pH3<sup>+</sup> mitotic cells in the ventricular zone (VZ) and subventricular zone (SVZ) of E15.5 WT and *Prdm16* cKO cortex.

(B) Number of PAX6<sup>+</sup> radial glia in E15.5 WT and *Prdm16* cKO cortex.

(C) Analysis of the timing of deep layer neurogenesis. EdU was injected at E14.5 and the percentage of CTIP2<sup>+</sup>/EdU<sup>+</sup> cells relative to total EdU<sup>+</sup> cells was quantified at E17.5 in WT and cKO cortex.

(D) Analysis of the timing of upper layer neurogenesis. EdU was injected at E17.5 followed by a second injection at post-natal day 0 (P0) and the total number of CUX1<sup>+</sup>, CUX1<sup>+</sup>/EdU<sup>+</sup> and CUX1<sup>+</sup>/EdU<sup>-</sup> cells was quantified at P2 in the white matter (WM) of WT and cKO cortex.

Quantification of pH3<sup>+</sup>, PAX6<sup>+</sup> and CTIP2<sup>+</sup>/EdU<sup>+</sup> cells was done in a 150  $\mu$ m-width column of the embryonic cortex (n=5). Results represent mean  $\pm$  SEM; statistical analysis is unpaired Student's t test (\*\*p < 0.001; n.s., not significant). Scale bars: 50  $\mu$ m (C), 250  $\mu$ m (D, low magnification) and 30  $\mu$ m (D, high magnification).

**Figure S6. Transcriptional profiling of sorted cortical cells. Related to Figure 4.**

(A) Expression of *NeuroD1*, *Dcx* and *Map2* in sorted radial glia, intermediate progenitors and neurons in E15.5 WT cortex. The intermediate progenitor population shows high levels of *NeuroD1* and *Dcx* expression and medium levels of *Map2* expression in comparison to more mature cortical neurons.

(B) Relative expression of *Prdm16* (exon 9) in sorted E15.5 WT and *Prdm16* cKO radial glia.

(C) Hierarchical clustering and principal component (PC) analysis of RNA sequencing data from four biological replicates sorted from E15.5 WT and *Prdm16* cKO cortex. Plots indicate that samples cluster by genotype, and most PC variance (64.2%) is explained by genotype.

(D) Real-time PCR analysis of 22 genes showing differential expression in RNA sequencing data from E15.5 WT and cKO radial glia. The relative gene expression was normalized using *Gapdh* as reference.

Results represent mean  $\pm$  SEM; statistical analysis is unpaired Student's t test (\*p < 0.05, \*\*p < 0.01, \*\*\*p < 0.001). RPKM: Reads Per Kilobase of transcript per Million mapped reads.

**Figure S7. Identification of PRDM16 binding sites, transcriptional targets and enhancer regulation. Related to Figures 5 and 6.**

(A) Comparison of the mean read density between PRDM16 ChIP-seq peaks in WT and *Prdm16* cKO cortex. The green dots represent differentially enriched binding sites (FDR < 0.05). The genome tracks show multiple PRDM16 binding sites at its own gene, whereas those peaks are absent in cKO cortex. Exon 9 of *Prdm16* is indicated.

(B) Genome tracks showing PRDM16 binding sites in proximity to *Insm1* and *Tbr2/Eomes*. The box plots indicate RNA-seq expression of *Insm1* and *Tbr2/Eomes* in E15.5 WT and cKO radial glia and intermediate progenitors (\*\*\* p < 0.001, n.s., not significant). RPKM: Reads Per Kilobase of transcript per Million mapped reads.

(C) Classification of PRDM16 binding sites into “developmental” or “developmental and adult” enhancers. The pie chart shows the number of each type of enhancer and the genome tracks show an example of H3K27ac enrichment for each type of enhancer.

**Figure S8. Upregulated genes in *Prdm16* cKO cortex are associated with increased H3K27ac. Related to Figure 6.**

(A) *Ptx3* expression in radial glia, intermediate progenitors and neurons was determined by RNA-seq in WT and *Prdm16* cKO cortex. Genome tracks show that *Ptx3* is the nearest gene to a PRDM16-bound enhancer showing increased H3K27ac in the cKO cortex (red box). The promoter region and gene body of *Ptx3* also show increased H3K27ac in the mutant cortex (purple box). The *Prdm16* cKO cortex displays increased levels of PTX3 in the ventricular zone (VZ), subventricular zone (SVZ) and intermediate zone (IZ).

(B) *Itga6* expression in radial glia, intermediate progenitors and neurons was determined by RNA-seq in WT and *Prdm16* cKO cortex. Genome tracks indicate that *Itga6* is the nearest gene to an upstream PRDM16-bound enhancer that shows increased H3K27ac in the cKO cortex (red box). The promoter region of *Itga6* also shows increased H3K27ac in the mutant cortex (purple box). Detection of *Itga6* transcripts by fluorescent *in situ* hybridization (FISH) shows up-regulated gene expression in the VZ, SVZ and IZ of E15.5 cKO cortex.

(C) *Gabra2* expression in radial glia, intermediate progenitors and neurons was determined by RNA-seq in WT and *Prdm16* cKO cortex. Genome tracks show an intronic region of *Gabra2* that is associated with two PRDM16-bound enhancers displaying an increase of H3K27ac in the cKO cortex (red boxes). Detection of *Gabra2* transcripts by FISH indicates up-regulated gene expression in the VZ, SVZ and IZ of E15.5 cKO cortex.

Quantification of FISH results is presented as the number of puncta (mean  $\pm$  SEM) in  $10^4 \mu\text{m}^2$  (n=3). To identify cortical neurons in the IZ, *Tubb3* expression was detected by FISH on the same tissue sections. The statistical analysis is unpaired Student's t test (\*p < 0.05, \*\*p < 0.01, \*\*\*p < 0.001). Scale bars: 200  $\mu\text{m}$  (A), 25  $\mu\text{m}$  (B, C).

**Figure S9. *Pdzn3* silencing by PRDM16 promotes cell migration. Related to figure 7.**

(A) *In vitro* knock-down (KD) of *Pdzrn3* expression by co-transfection of HEK293 cells with a plasmid encoding *Pdzrn3* in combination with scrambled RNA control (*Pdzrn3* scrRNA) or *Pdzrn3* short hairpin RNA (*Pdzrn3* shRNA). Two days after transfection, the relative expression of *Pdzrn3* was determined by real-time PCR analysis.

(B, C) Analysis of cell migration after single KD of *Prdm16* or double KD of *Prdm16* and *Pdzrn3*. Vectors coding for shRNA or scrRNA were co-electroporated with a vector encoding nuclear *GFP*. *In utero* electroporations were done at E14.5 and the fraction of *GFP*<sup>+</sup> cells was quantified in four bins comprising the cerebral cortex and white matter at post-natal day 5 (P5)(n=3, *Prdm16* scrRNA; n=4, *Prdm16* shRNA; n=5, *Prdm16* shRNA and *Pdzrn3* scrRNA; n=7, *Prdm16* shRNA and *Pdzrn3* shRNA).

(D) A plasmid encoding *Pdzrn3* upstream *GFP* or a control *GFP* empty vector were electroporated into E14.5 brains followed by analysis of neuronal migration at P5. Over-expression of *Pdzrn3* resulted in many ectopic *CUX1*<sup>+</sup> neurons in 4 out of 8 brains, whereas 0 out of 5 electroporated brains with the control vector resulted in ectopic cortical neurons (n=4 independent electroporation experiments).

(E) PDZRN3 immunostaining of cells electroporated with the vector encoding *Pdzrn3*. Inset images show in greater detail ectopic PDZRN3<sup>+</sup> neurons near the white matter.

Results represent mean ± SEM; statistical analysis is unpaired Student's t test (\*p < 0.05, \*\*p < 0.01, \*\*\*p < 0.001; n.s. not significant). Scale bars: 100 μm (B, D and E), and 50 μm (E, inset images).

**Figure S10. The histone methyl-transferase domain of PRDM16 promotes cell migration.**

**Related to figure 8.**

(A, B) *In utero* electroporations (IUE) of control, *Hes5p-Prdm16* F.L and *Hes5p-ΔPRdm16* vectors into E13.5 WT or *Prdm16* cKO cortex. Experimental vectors were co-electroporated with a plasmid encoding nuclear *GFP*. The fraction of *GFP*<sup>+</sup> nuclei was quantified in four bins

comprising the cortical plate (CP), intermediate zone (IZ) and white matter (WM) in E18.5 cortex (n=6, control vector in *Prdm16* WT; n=3, control vector in *Prdm16* cKO; n=3, *Prdm16* F.L in *Prdm16* cKO; n=5,  $\Delta PRdm16$  in *Prdm16* cKO).

Results represent mean  $\pm$  SEM; statistical analysis is unpaired Student's t test (\*p < 0.05; n.s. not significant). Scale bar: 50  $\mu$ m (A).



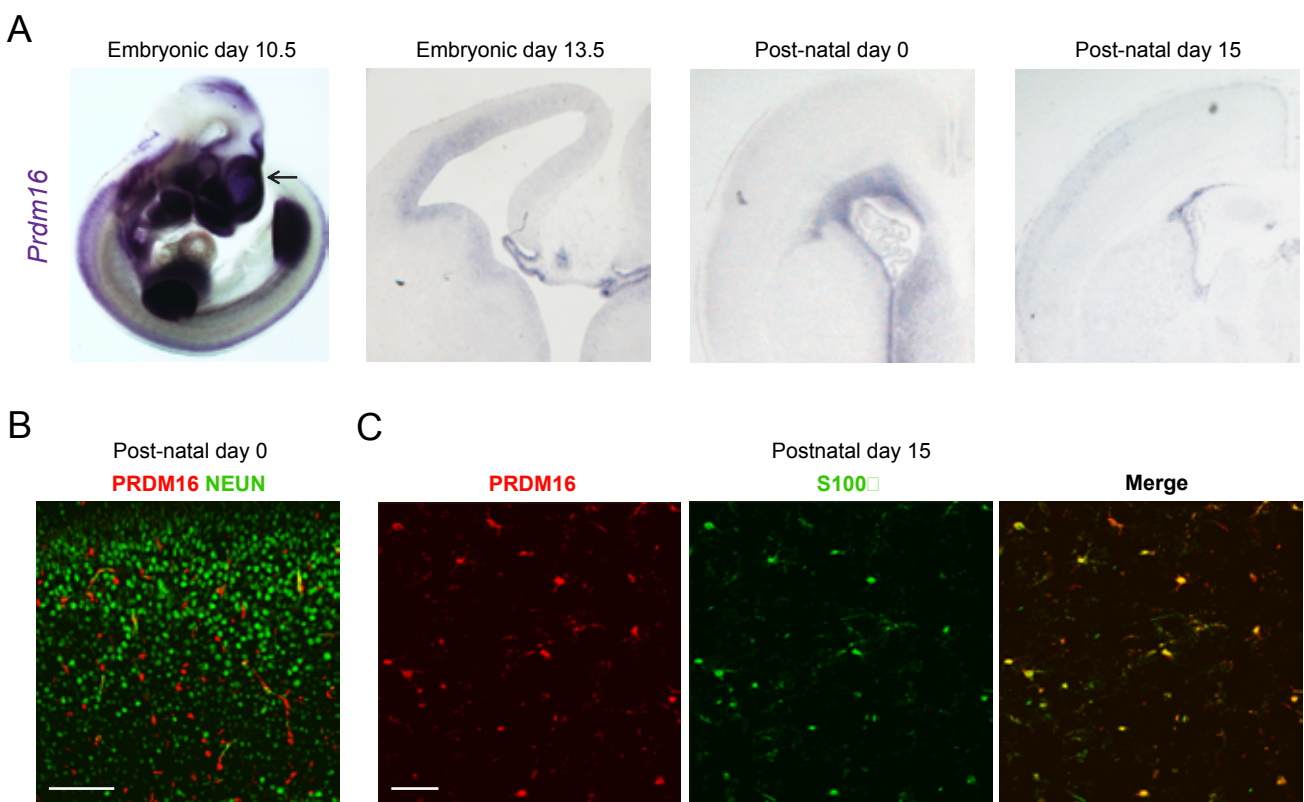


Figure S1. Related to Figure 1.

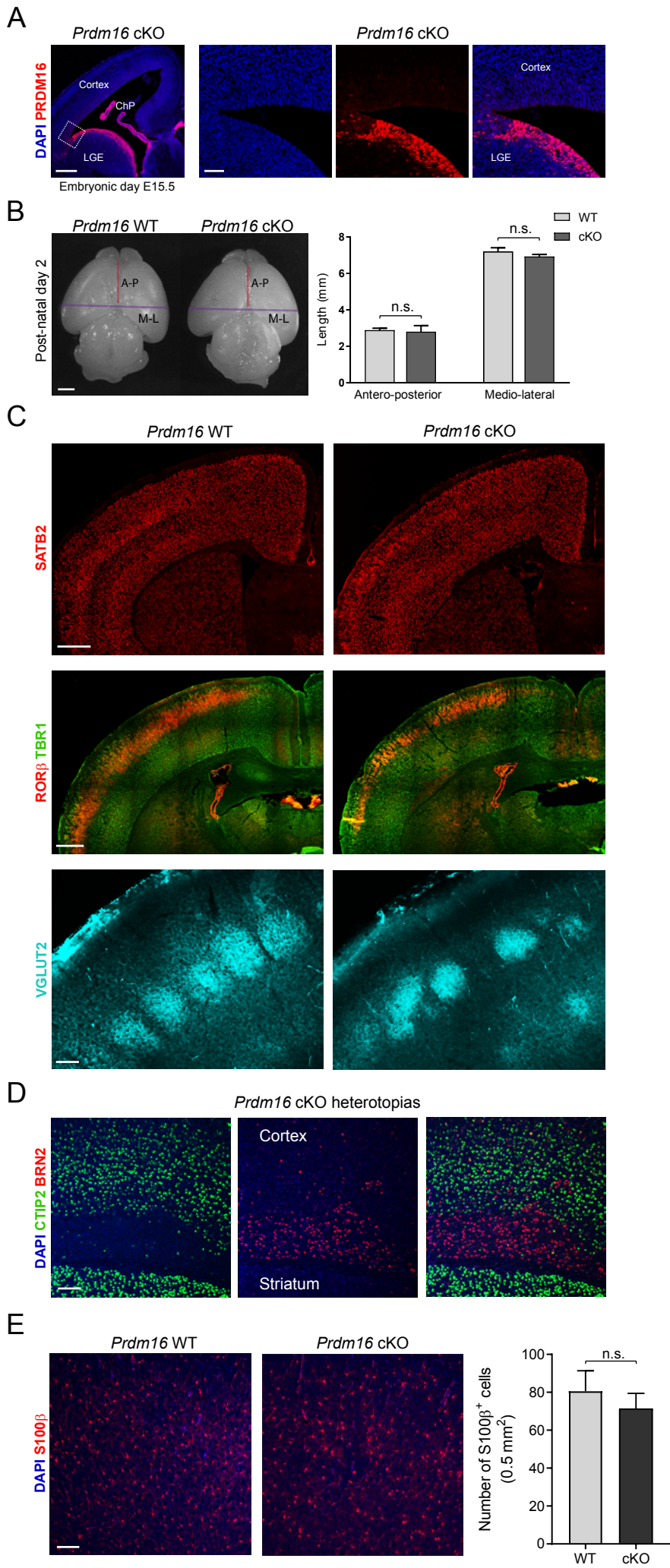


Figure S2 Related to Figure 2.

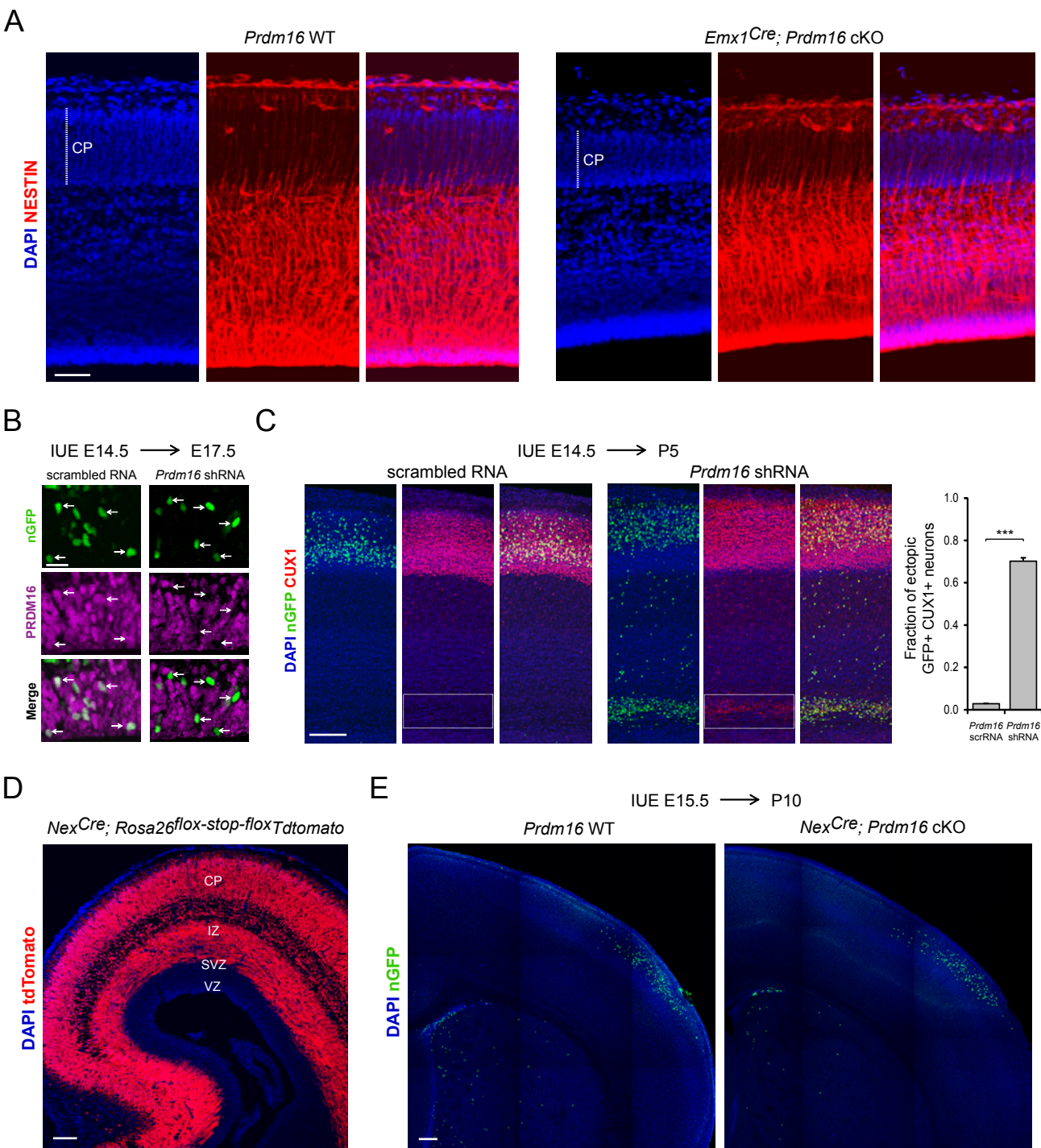
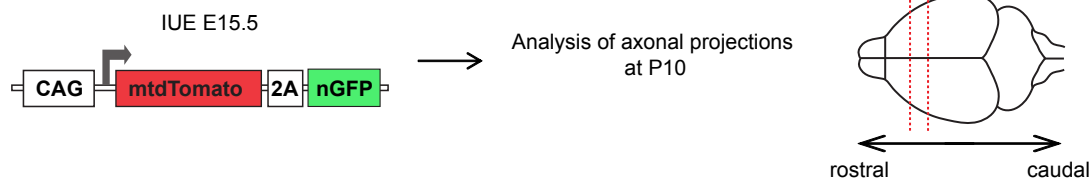
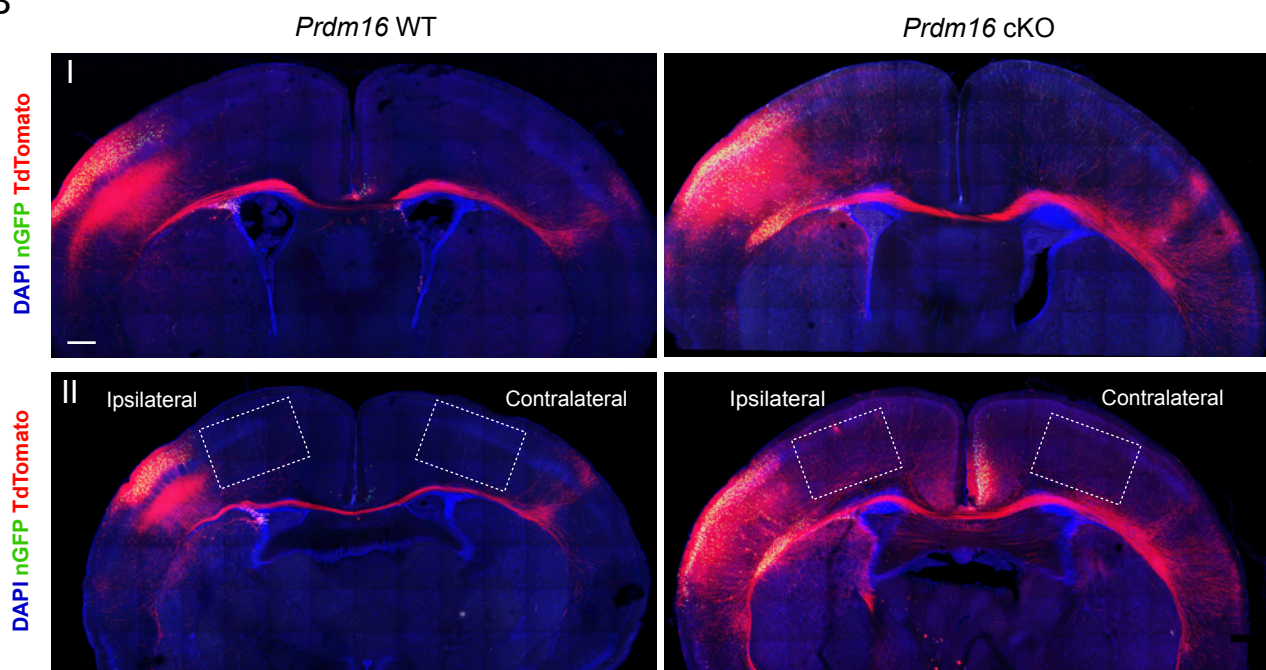


Figure S3. Related to Figure 2.

A



B



C

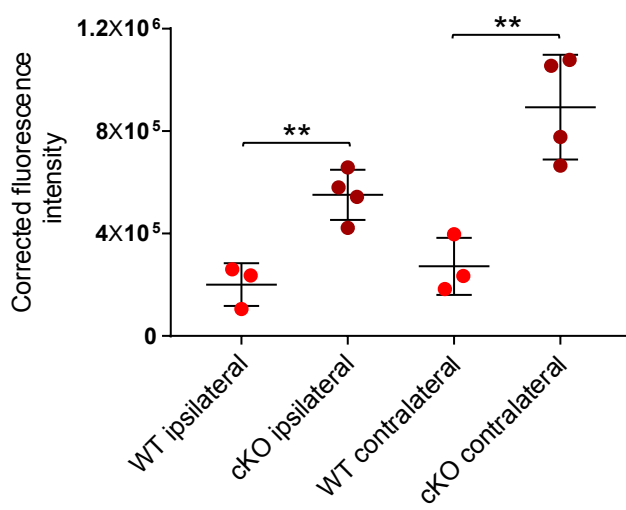


Figure S4. Related to Figure 2.

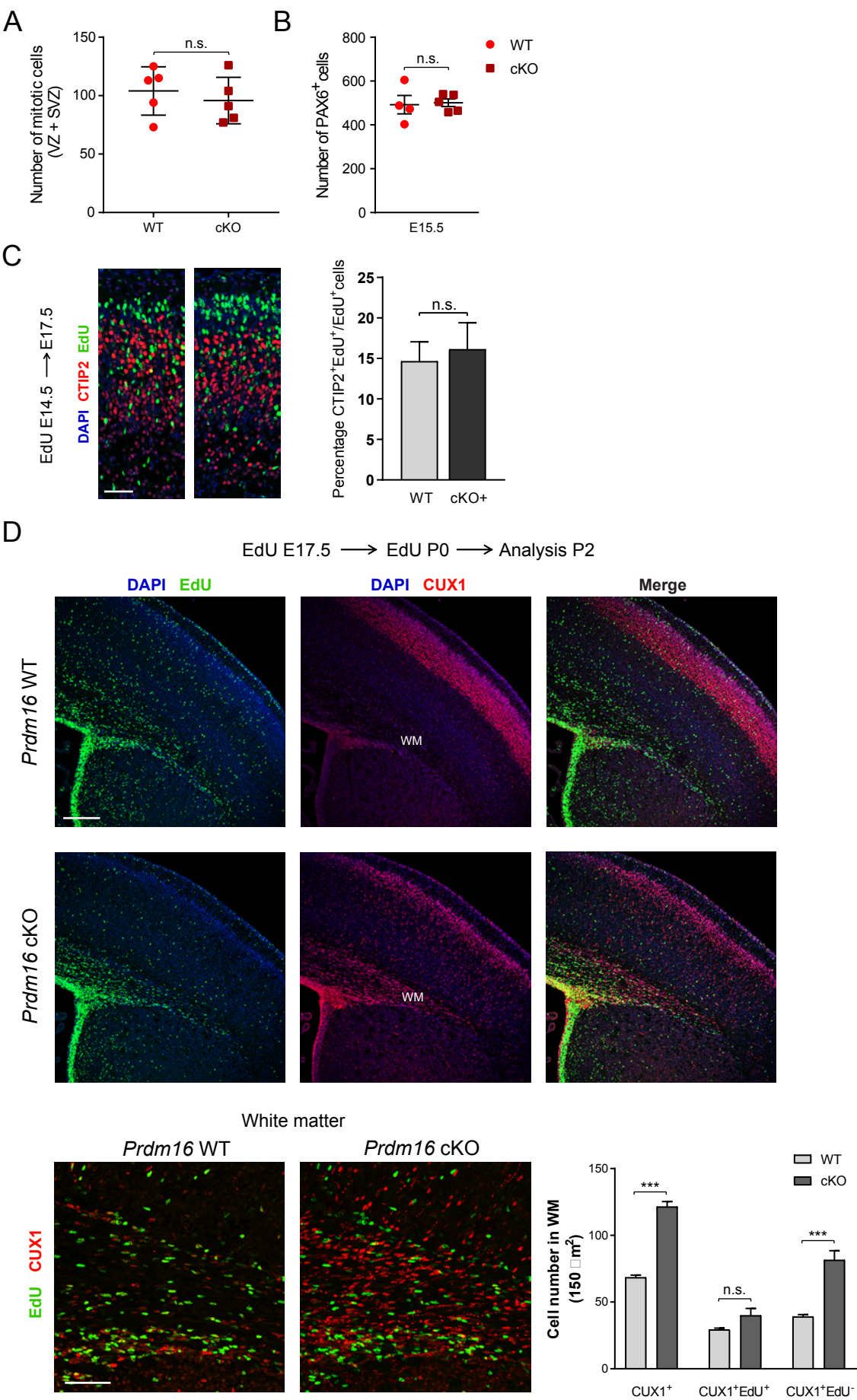
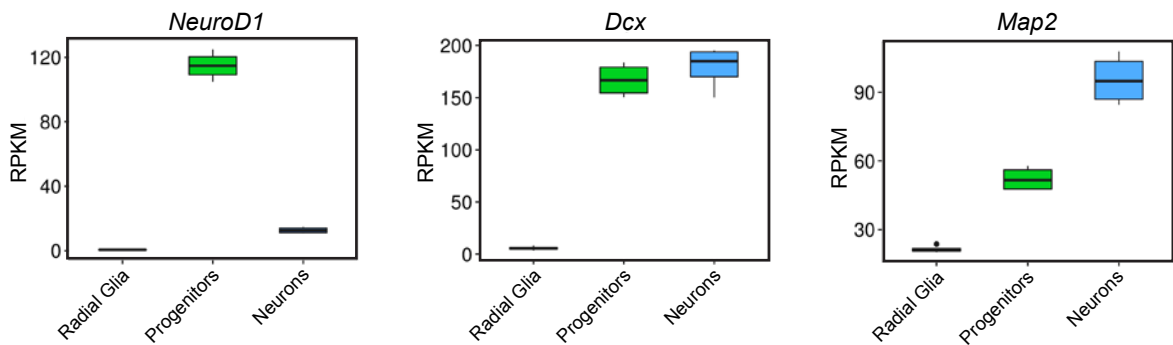
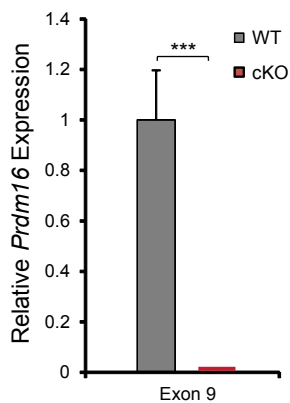


Figure S5. Related to Figure 3.

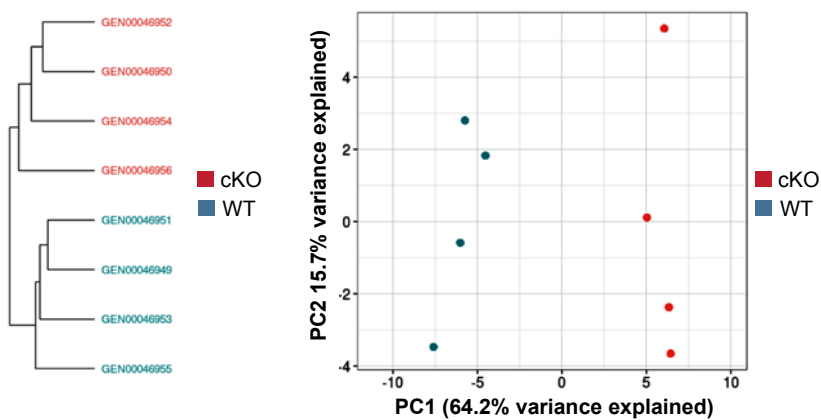
A



B



C



D

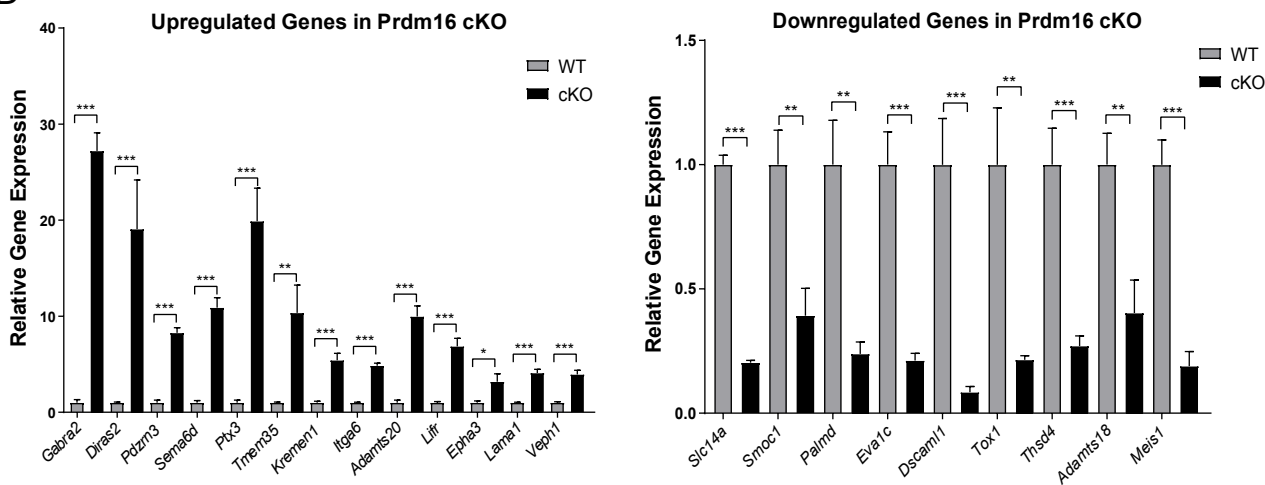


Figure S6. Related to Figure 4.

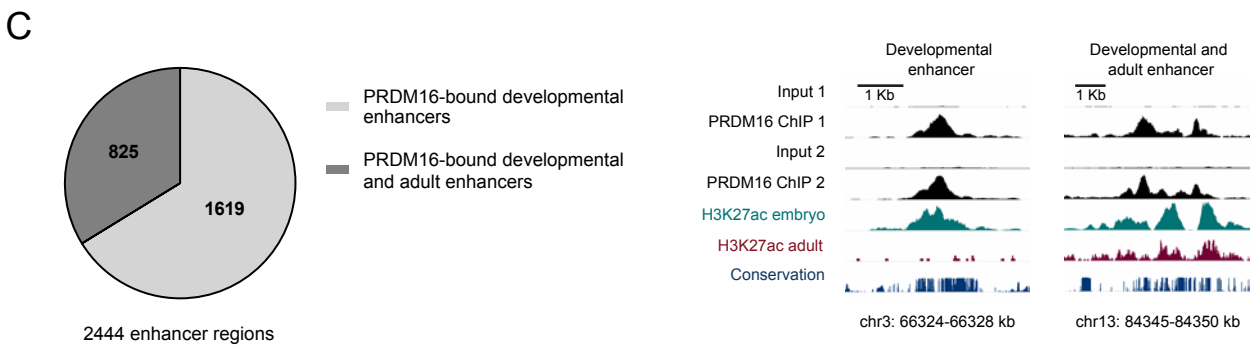
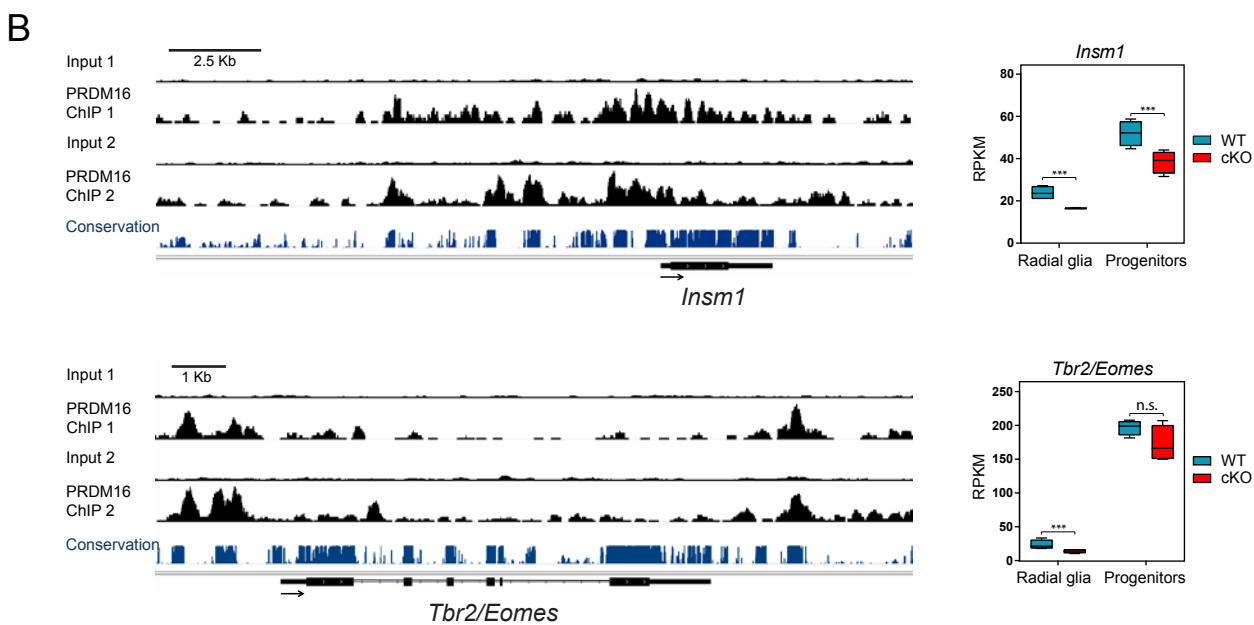
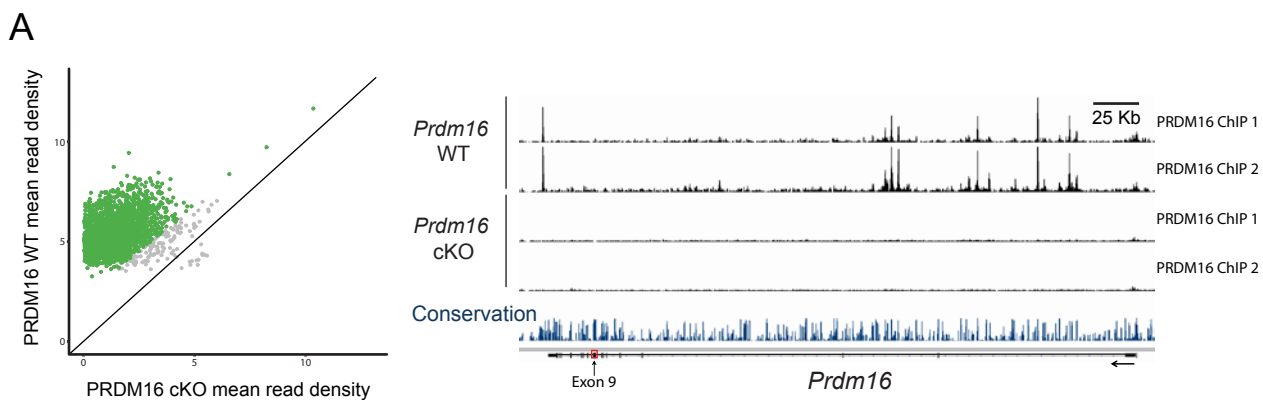


Figure S7. Related to Figures 5 and 6.

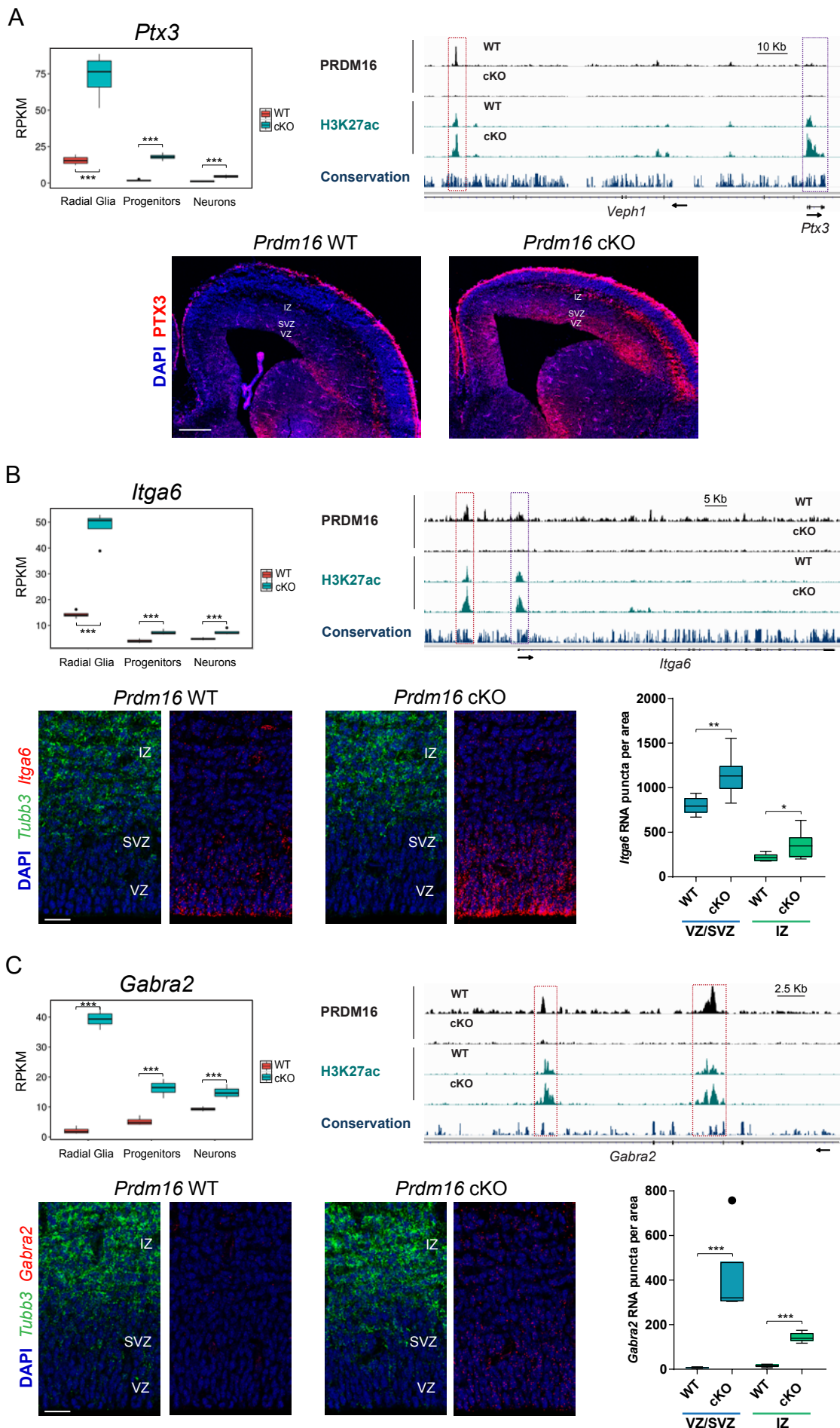


Figure S8. Related to Figure 6.





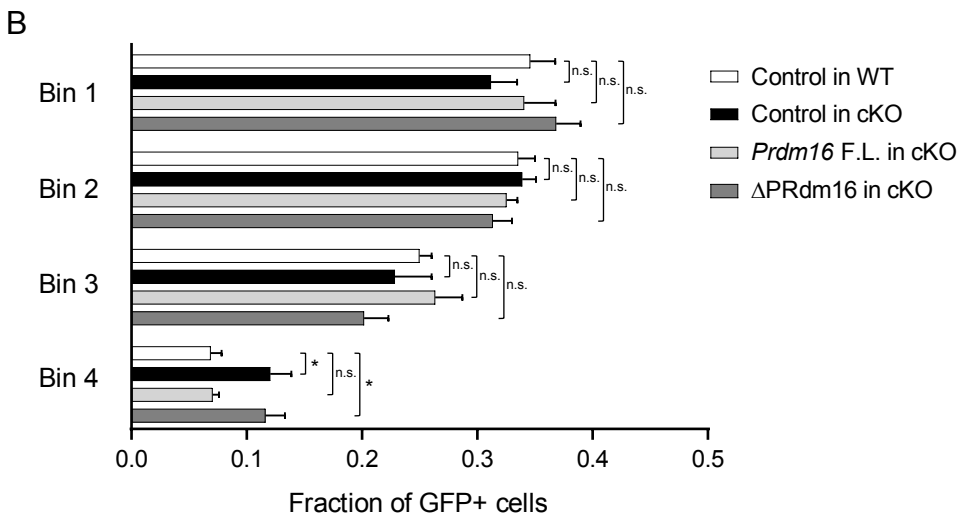
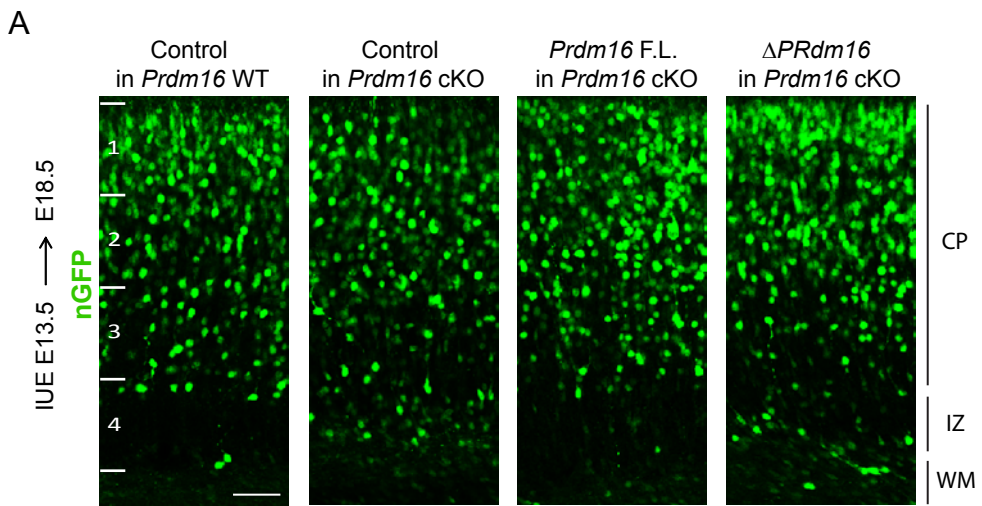


Figure S10. Related to Figure 8.